© 2021. Published by The Company of Biologists Ltd | Journal of Cell Science (2021) 134, jcs253559. doi:10.1242/jcs.253559

RESEARCH ARTICLE

Identification of a heat-inducible novel nuclear body containing the long noncoding RNA *MALAT1*

Rena Onoguchi-Mizutani[1], Yoshitaka Kirikae[1], Yoko Ogura[1], Tony Gutschner[2], Sven Diederichs[3,4] and Nobuyoshi Akimitsu[1,*]

ABSTRACT

The heat-shock response is critical for the survival of all organisms. Metastasis-associated long adenocarcinoma transcript 1 (*MALAT1*) is a long noncoding RNA localized in nuclear speckles, but its physiological role remains elusive. Here, we show that heat shock induces translocation of *MALAT1* to a distinct nuclear body named the heat shock-inducible noncoding RNA-containing nuclear (HiNoCo) body in mammalian cells. *MALAT1*-knockout A549 cells showed reduced proliferation after heat shock. The HiNoCo body, which is formed adjacent to nuclear speckles, is distinct from any other known nuclear bodies, including the nuclear stress body, Cajal body, germs, paraspeckles, nucleoli and promyelocytic leukemia body. The formation of HiNoCo body is reversible and independent of heat shock factor 1, the master transcription regulator of the heat-shock response. Our results suggest the HiNoCo body participates in heat shock factor 1-independent heat-shock responses in mammalian cells.

KEY WORDS: Heat-shock response, Nuclear body, Long noncoding RNA, MALAT1

INTRODUCTION

Heat shock causes protein unfolding and nonspecific aggregation that cause proteotoxicity (Richter et al., 2010). The heat-shock response (HSR) is an evolutionarily conserved cellular defense mechanism for eliminating proteotoxicity and maintaining protein homeostasis (proteostasis). The HSR induces transcription of multiple gene products, including molecular chaperones, which assist protein folding. Heat shock factor 1 (HSF1) is a critical transcription factor in the HSR, and induces target genes, such as the chaperone genes (Li et al., 2017). The HSF1–chaperone axis is considered the central HSR in that it increases protein folding capacity and rebalances proteostasis, thereby supporting cell survival. However, a recent genome-wide analysis of transcriptional regulation using *HSF1*-knockout cells revealed that HSR acts not only through HSF1-dependent transcriptional activation but also through HSF1-independent transcriptional regulation (Mahat et al., 2016).

[1]Isotope Science Center, The University of Tokyo, Tokyo, 113-0032, Japan. [2]Junior Research Group 'RNA Biology and Pathogenesis', Medical Faculty, Martin-Luther University Halle-Wittenberg, 06120 Halle/Saale, Germany. [3]Division of Cancer Research, Department of Thoracic Surgery, Medical Center - University of Freiburg, Faculty of Medicine, University of Freiburg, German Cancer Consortium (DKTK) - Partner Site Freiburg, 79106 Freiburg, Germany. [4]Division of RNA Biology & Cancer, German Cancer Research Center (DKFZ), 69120 Heidelberg, Germany.

*Author for correspondence (akimitsu@ric.u-tokyo.ac.jp)

N.A., 0000-0002-3190-2942

Handling Editor: Maria Carmo-Fonseca
Received 26 August 2020; Accepted 29 March 2021

The cell nucleus contains many nuclear bodies, which are composed of specific proteins and RNAs (Banani et al., 2017; Hyman et al., 2014). Nuclear bodies show liquid-like properties that arise through liquid–liquid phase separation (Banani et al., 2017; Hyman et al., 2014). Nuclear bodies also contribute to cellular stress responses. For example, a nuclear stress body is formed upon heat shock in an HSF1-dependent manner (Cotto et al., 1997; Jolly et al., 1999) and regulates the intron retention of various pre-mRNAs in heat-shocked cells (Ninomiya et al., 2020).

Long noncoding RNAs (lncRNAs) are transcripts that lack obvious protein coding potential and regulate gene expression (Engreitz et al., 2016; Shirahama et al., 2020). A subset of lncRNAs are components of nuclear bodies (Hirose et al., 2019). *NEAT1* is an lncRNA essential for forming the nuclear body, paraspeckle (Clemson et al., 2009), and plays an important role in the cellular immune response to pathogenic infection (Imamura et al., 2014, 2018). Metastasis associated lung adenocarcinoma transcript 1 (*MALAT1*) is a component of other nuclear bodies, termed nuclear speckles, which are composed of pre-mRNA splicing and transcription factors (Hutchinson et al., 2007; Miyagawa et al., 2012). *MALAT1* was originally identified as a prognostic marker of metastasis and patient survival in non-small cell lung carcinoma (Ji et al., 2003). We have reported that *MALAT1* promotes cell migration through regulation of cell migration-related gene expression at the transcriptional level (Tano et al., 2010) and that it represses transcription of the p53 gene (*TP53*) (Tano et al., 2018). *MALAT1* also regulates alternative splicing by regulating splicing factors in nuclear speckles (Tripathi et al., 2010). These studies suggest that *MALAT1* contributes to cancer progression and metastasis through regulation of gene expression (Arun et al., 2020). Despite the importance of *MALAT1* in gene regulation in cancer, *Malat1*-knockout mice show no obvious phenotype under regular breeding conditions (Eißmann et al., 2012; Nakagawa et al., 2012; Zhang et al., 2012). Hence, the physiological function of *MALAT1* is an open question to date.

In this study, we showed that *MALAT1* translocates in response to heat shock from nuclear speckles to a distinct granule-like structure, named heat-inducible noncoding RNA-containing nuclear body (HiNoCo body), in an HSF1-independent manner.

RESULTS

MALAT1 localization alters in response to heat shock

We examined the nuclear localization of *MALAT1* in response to heat shock by RNA fluorescence *in situ* hybridization (FISH). Under control conditions, *MALAT1* was localized in nuclear speckles probed by immunofluorescence staining of the core components, SRSF2 and SRRM2, in human alveolar adenocarcinoma cell line A549 cells (Fig. 1A; Fig. S1A). Heat treatment at 42°C induced the translocation of *MALAT1* from nuclear speckles to granule-like structures adjacent to the nuclear speckles (Fig. 1A).

Journal of Cell Science (2021) 134, jcs253559. doi:10.1242/jcs.253559

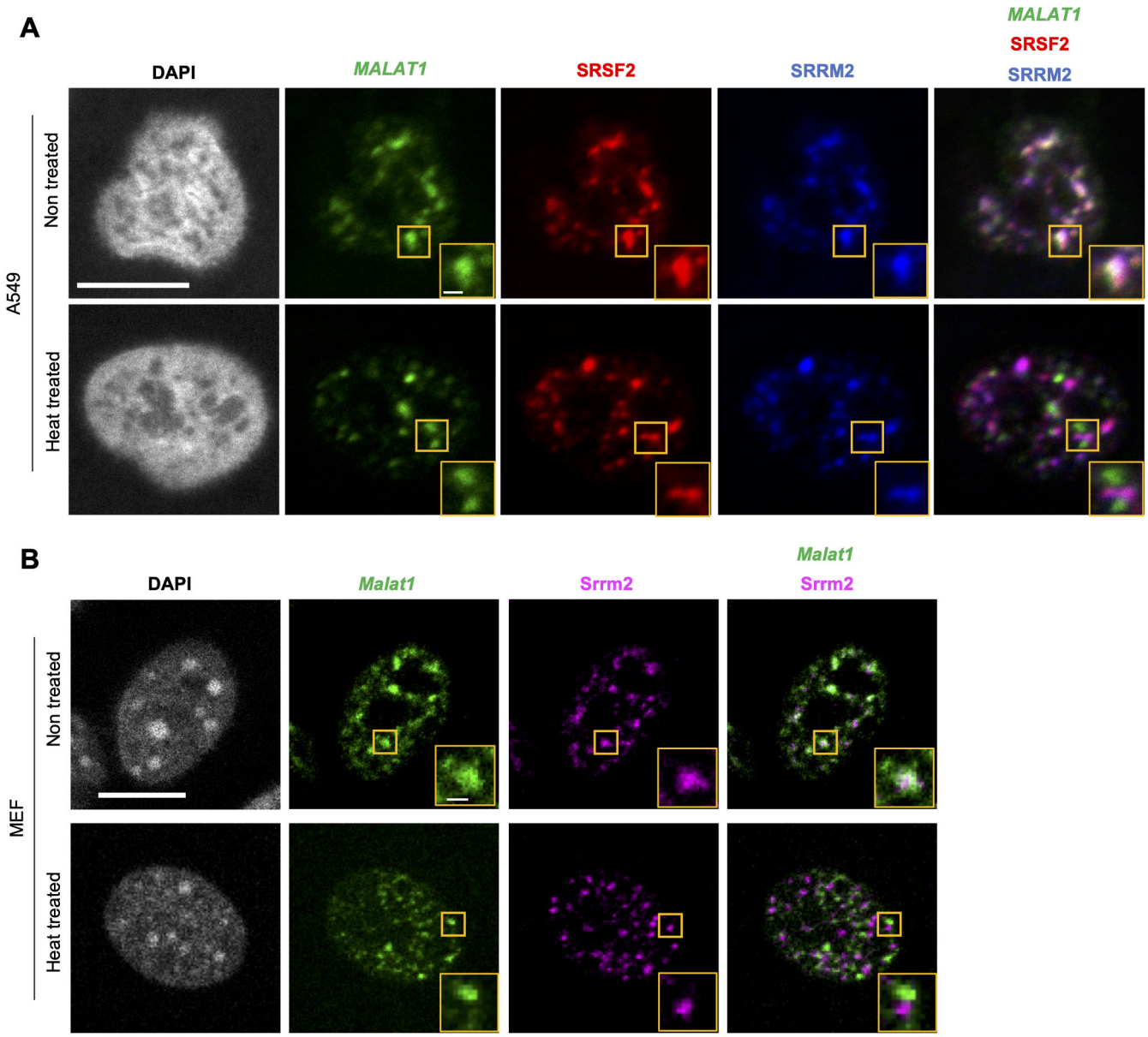

Fig. 1. Altered localization of *MALAT1* in heat-treated mammalian cells. Representative images of *MALAT1* lncRNA and nuclear speckle proteins in cells exposed to 42°C for 1 h. (A) Heat-treated A549 cells were subjected to RNA-FISH for *MALAT1* (green), and to immunofluorescence staining for SRSF2 (red) and SRRM2 (blue). DAPI was used for nuclei visualization. (B) Heat-treated mouse embryonic fibroblasts (MEFs) were examined by RNA-FISH for *Malat1* (green) and immunofluorescence staining for Srrm2 (red). DAPI was used for nuclei visualization. Scale bars: 10 µm (main images), 1 µm (enlarged images at the bottom right).

We analyzed whether other stresses also induced the translocation of *MALAT1* into granule-like structures adjacent to the nuclear speckles. Sodium arsenate treatment led to *MALAT1* redistributing to two locations; primarily a diffusion into the nucleoplasm and with a minor localization in stress bodies marked by G3BP (also known as G3BP1), a stress body marker protein (Fig. S1D,E). Ultraviolet irradiation caused the diffusion of *MALAT1* into the nucleoplasm, with a small granule-like pattern (Fig. S1F). *MALAT1* was mainly localized in nuclear speckles but a significant amount was diffused into the nucleoplasm with a small granule-like pattern seen in X-ray-irradiated cells (Fig. S1F). As shown in previous reports (Bernard et al., 2010; Tani et al., 2012a), transcriptional inhibition by actinomycin D caused *MALAT1* to diffuse into nucleoplasm. Thus, heat shock induced a distinct localization of *MALAT1* in the nucleus.

Next, we investigated whether transcriptional inhibition affects *MALAT1* translocation into the granule-like structures under heat shock. As shown in Fig. S1G, transcriptional inhibition by actinomycin D or 5,6-dichloro-β-D-ribofuranosylbenzimidazole (DRB) led to *MALAT1* diffusion into the nucleoplasm with small granule-like particles spreading throughout the nucleoplasm under heat shock (Fig. S1G).

To further investigate the *MALAT1*-containing granule-like structures, we examined the localization of SON and SRSF3, typical nuclear speckle proteins (Fig. S2A) (Sharma et al., 2010; Tripathi et al., 2012). Under heat shock, SON was colocalized with SRSF2. A large amount of SRSF3 was diffuse in the nucleoplasm and a small amount of SRSF3 overlapped with both SRSF2 and *MALAT1* in the control and heat-treated A549 cells (Fig. S2A). The number of MALAT1-containing granule-like structures was

Journal of Cell Science (2021) 134, jcs253559. doi:10.1242/jcs.253559

significantly fewer than the number of nuclear speckles in heat-treated cells (Fig. S2B). A previous study has reported that nuclear speckles have a multi-layered structure (Fei et al., 2017). By using high-resolution imaging with deconvolution, we confirmed that SRSF2 and SON were centered in nuclear speckles and that *MALAT1* was present around SRSF2 and SON (Fig. S2C). *MALAT1* showed a relatively homogenous distribution in the granule-like structures under heat shock (Fig. S2C).

The heat shock-mediated translocation of *MALAT1* was also observed in mouse embryonic fibroblasts (MEFs; Fig. 1B; Fig. S1B) and mouse C17.2 cells (Fig. S1C), indicating that the heat shock-induced change in the *MALAT1* nuclear localization is evolutionarily conserved and occurs in normal primary cells as well as in cancer-derived cells.

To investigate whether the heat-shock-induced translocation of *MALAT1* is mediated by either pre-existing or newly synthesized *MALAT1*, we measured *MALAT1* RNA turnover upon heat shock through immunoprecipitation of pulse-labeled RNA with bromouridine (BrU), followed by reverse transcription quantitative real-time PCR (qRT-PCR) (Fig. 2A). The overall amount of *ACTB* mRNA, *MYC* mRNA and *MALAT1* lncRNA did not change upon heat shock, whereas the *HSPB1* mRNA level increased by 3.4-fold ($P<0.01$; Fig. 2B). At 1 h post pulse-labeling, the recovered BrU-labeled *ACTB* mRNA, *HSPB1* mRNA and *MALAT1* lncRNA did not significantly reduce in both the control and heat-shock groups, indicating that these RNAs are stable and that most of them pre-existed at 1 h after heat shock (Fig. 2B,C). In contrast, the recovered BrU-labeled *MYC* mRNA was reduced to 20% ($P<0.01$) in both the control and heat-shock groups, indicating that *MYC* mRNA has a high turnover rate and that most of the *MYC* mRNA was newly synthesized mRNA at 1 h after heat shock (Fig. 2B,C). Northern blot analysis showed that the length and amount of *MALAT1* were not altered in heat-shocked cells (Fig. 2D). We investigated whether heat shock affected the processing of *MALAT1*-associated small cytoplasmic RNA (mascRNA), a tRNA-like transcript generated from the 3′ end of *MALAT1* RNA (Wilusz et al., 2008). There was no significant difference in the expression level of unprocessed *MALAT1* in non-treated and heat-treated A549 cells, indicating heat shock does not alter the mascRNA processing from *MALAT1* (Fig. S2D,E). These results show that heat shock changes the nuclear localization of *MALAT1* from nuclear speckles to other nuclear structures without changing its expression level, processing and turnover rate.

To determine the biological significance of *MALAT1* in the HSR, we examined the cell proliferation of wild-type and *MALAT1*-knockout A549 cells with or without heat shock treatment. Under control conditions, there was no significant difference in cell proliferation between wild-type and *MALAT1*-knockout A549 cells (Fig. 2E). However, the cell proliferation of *MALAT1*-knockout A549 cells was reduced after heat shock, compared with heat-treated wild-type cells. This suggests that *MALAT1* is important for the HSR.

Formation of novel heat-inducible noncoding RNA *MALAT1*-containing nuclear bodies in an HSF1-independent manner

Co-staining of *MALAT1* and marker proteins of known nuclear bodies in A549 cells after heat shock showed that *MALAT1* was not colocalized with any known nuclear bodies, such as nuclear stress body, paraspeckles, Cajal body, nucleoli, gems and promyelocytic leukemia bodies labeled by HSF1, SFPQ, coilin, FBL, SMN1 and PML, respectively (Fig. 3A). These results indicate that heat shock induces the translocation of *MALAT1* from nuclear speckles to a distinct nuclear body. We named this *MALAT1*-containing nuclear body heat-inducible noncoding RNA-containing nuclear body, with the acronym HiNoCo, which means fire spark in Japanese.

HSF1 is the master transcription regulator of the HSR (Li et al., 2017). We therefore examined the formation of HiNoCo-bodies in HSF1-knockdown cells (Fig. 3B,C). HSF1 knockdown was confirmed by qRT-PCR and western blotting (Fig. 3B), in which HSF1 mRNA and protein decreased to less than 10% of that in control cells. Heat shock increased *HSPB1* mRNA expression, which is controlled by HSF1 (Trinklein et al., 2004), by 3.5-fold in control cells, but it was unchanged in HSF1-knockdown cells (Fig. 3C), indicating that functional knockdown of HSF1 was successfully established. The *MALAT1* RNA level was unchanged in HSF1-knockdown cells before and after heat shock (Fig. 3C). The formation of HiNoCo bodies probed by *MALAT1* was similar in control and HSF1-knockdown cells (Fig. 3D), and the size of HiNoCo bodies was not significantly altered in HSF1-depleted cells (Fig. 3E), indicating HiNoCo body is formed through an HSF1-independent mechanism.

To get an insight in the protein factor(s) of the HiNoCo body, we performed knockdown experiments using previously reported protein factors that affected *MALAT1* localization in nuclear speckles (Miyagawa et al., 2012; Tripathi et al., 2010; Wang et al., 2019). The knockdown of SRRM1, RNPS1, DHX15, SON, DDX42, HNRNPH1 and HNRNPK, which have been reported to negatively regulate the nuclear speckle localization of *MALAT1*, promoted the diffusion of *MALAT1* in the nucleoplasm of non-treated and heat-treated A549 cells (Fig. S3). Unlike previous studies, the knockdown of PRP6 did not cause the disruption of nuclear speckle localization of *MALAT1* in non-treated A549 cells, but promoted the diffusion of *MALAT1* into the nucleoplasm in heat-treated A549 cells (Fig. S3). However, PCBP1 knockdown caused the retention of *MALAT1* in nuclear speckles even under heat shock (Fig. S3). These results indicate that PCBP1 is required for the relocation of *MALAT1* from nuclear speckles in response to heat shock.

Time course of HiNoCo body formation after heat shock

Examining the time course of HiNoCo body formation after heat shock at 42°C (Fig. 4A,B) revealed that *MALAT1* started to diffuse from nuclear speckles into the nucleoplasm at 5 min and diffused mostly in the nucleus at 10 and 15 min. *MALAT1* formed small granules at 30 min and large HiNoCo bodies at 60 min. Even after 3 h of heat shock, HiNoCo bodies remained within the nucleus, although the size of these bodies tended to be smaller than they were 1 h after heat shock (Fig. S4A).

When the incubation temperature was changed from 42°C to 37°C, the *MALAT1* was not localized in nuclear speckles at 10 min after the temperature shift, but it partially returned to the nuclear speckles 30 min after recovery and completely after 60 min of recovery (Fig. 4A,B). Quantitative analysis using LAS-AF software clearly showed that *MALAT1* exited from nuclear speckles in response to heat shock and it returned to nuclear speckles after reducing the temperature back to 37°C (Fig. 4B). When a second heat shock at 42°C was applied after 60 min of recovery, *MALAT1* again formed HiNoCo bodies (Fig. S4B). *MALAT1* localization was not altered at 10 min after the change in incubation temperature from 42°C to 37°C after the second heat shock treatment, but returned to nuclear speckles 30 min after recovery similar to the first recovery step (Fig. S4B).

Poly(A)+ RNA was localized in nuclear speckles at every time point of the heat shock and the recovery step (Fig. S4C). We also found that *U1snRNA* was colocalized with nuclear speckles in the non-treated and

Journal of Cell Science (2021) 134, jcs253559. doi:10.1242/jcs.253559

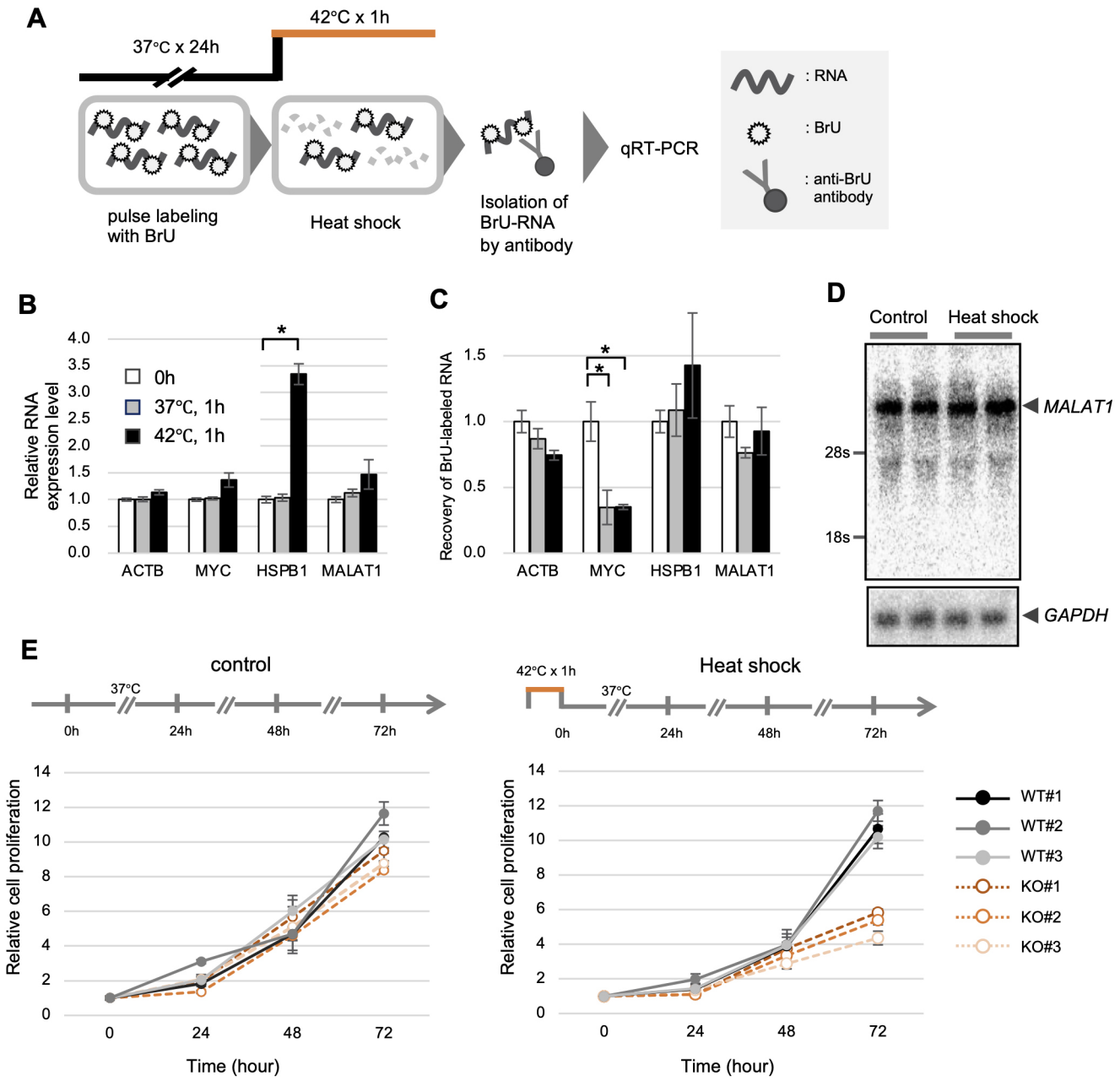

Fig. 2. Determination of turnover and length of *MALAT1* in heat-treated cells. (A) Schematic illustration of the experimental design for examining *MALAT1* turnover by a pulse-chase experiment. After BrU pulse-labeling, A549 cells were incubated at 37°C or 42°C for 1 h. BrU-labeled RNA was purified from isolated total RNA by means of anti-BrU antibody, followed by qRT-PCR. (B) The relative expression levels (before immunoprecipitation) of the indicated RNAs in cells at time 0 after BrU pulse-labeling (white bars), and after 1 h at 37°C (gray bars) or 42°C (black bars) were determined by qRT-PCR. The RNA expression level was normalized to *GAPDH* mRNA. (C) qRT-PCR was used to determine the recovery of BrU-labeled RNA at time 0 (white bar), 37°C for 1 h (gray bar), and 42°C for 1 h (black bar). In B and C, the results are presented as a relative value normalized to the level of *GAPDH* (mean±s.d.) of biological triplicates, and the RNA level at 0 h was set to 1. **P*<0.01 (Welch's *t*-test). (D) Northern blot analysis showed *MALAT1* and *GAPDH* mRNA in non-treated and heat-treated A549 cells using the indicated probes. Each condition had two duplicates. (E) Wild-type cells A549 (WT) and *MALAT1*-knockout A549 cells (KO) were incubated at 37°C or 42°C for 1 h, and the proportion of viable cells were quantified at 0, 24, 48, and 72 h using Cell Counting Kit-8 (*n*=4) and is presented as a relative value (mean±s.d.). Representative data from two independent experiments are shown.

heat-treated cells (Fig. S4D), indicating that the formation of the HiNoCo body is specific for *MALAT1*, but not for poly(A)+ RNA and *U1snRNA*.

Inhibition of HiNoCo body formation upon 1,6-hexanediol treatment

HiNoCo bodies showed a granule-like shape that is a typical shape of phase-separated structures (Hyman et al., 2014). HiNoCo bodies gradually grow over time upon stress (Fig. 4A), similar to what is seen for stress granules, which are cytoplasmic phase-separated structures (Wheeler et al., 2016). We therefore hypothesized that the HiNoCo body is formed by liquid–liquid phase separation.

The HiNoCo body granules containing *MALAT1* in heat-shocked cells disintegrated upon treatment with 1,6-hexanediol (Fig. 5A), an

Journal of Cell Science (2021) 134, jcs253559. doi:10.1242/jcs.253559

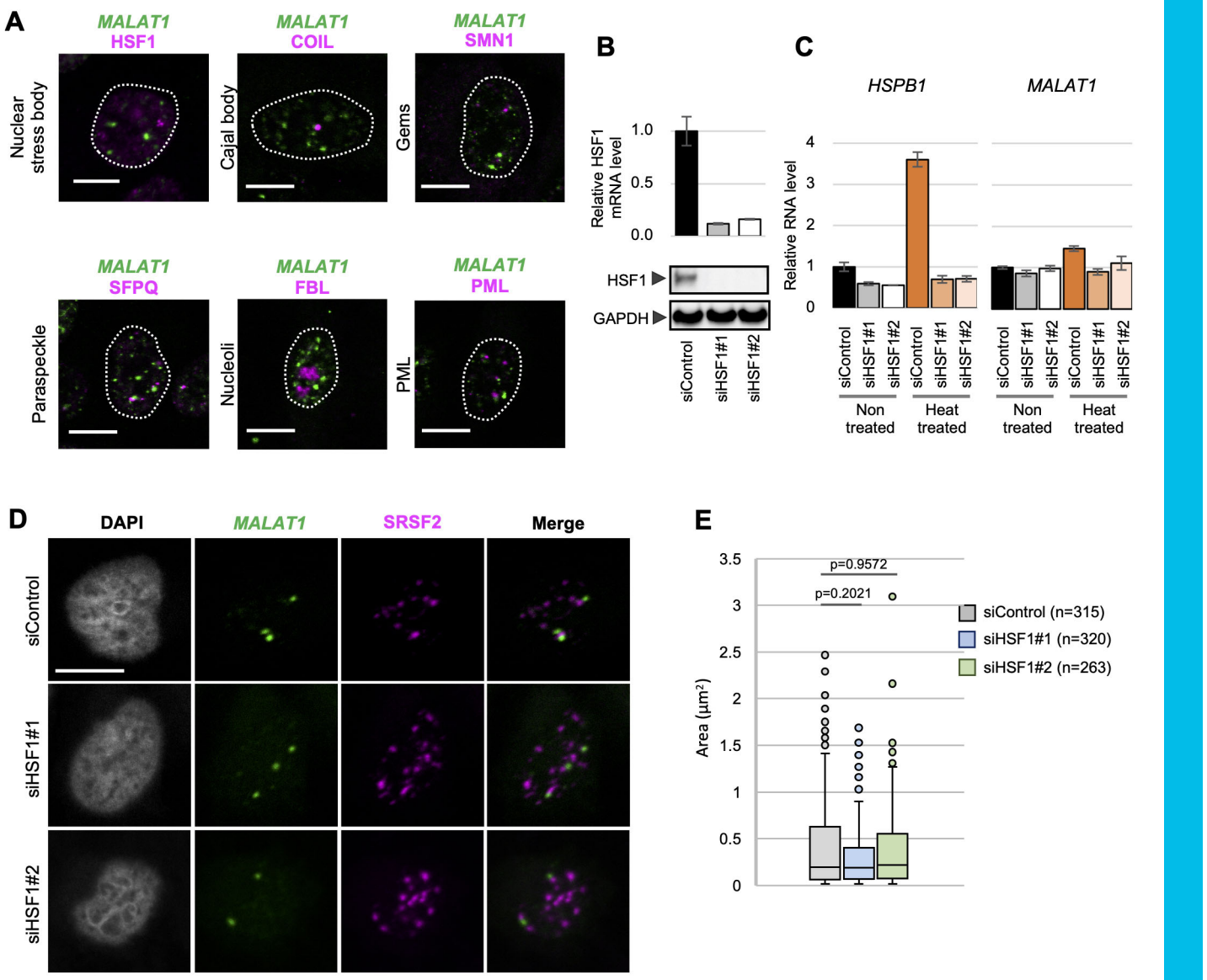

Fig. 3. Localization of *MALAT1* and known nuclear bodies in heat-treated cells. (A) A549 cells were incubated at 42°C for 1 h, followed by RNA-FISH staining and immunostaining using specific antibodies against the indicated marker proteins. Merged images of *MALAT1* (green) and the indicated nuclear body marker protein (magenta) in heat-treated A549 cells are shown. Dotted lines outline the nucleus. Scale bars: 10 µm. (B) qRT-PCR (upper) and western blot (lower) data showing the knockdown efficiency of HSF1 in A549 cells. (C) The relative RNA expression level compared to the control knockdown (siControl) was determined by qRT-PCR. In B and C, each RNA level was normalized to *GAPDH* mRNA and mean±s.d. was determined for biological triplicates. (D) Representative images of *MALAT1* RNA and nuclear speckle proteins in heat-treated HSF1-knockdown cells. RNA-FISH analysis of *MALAT1* (green) in A549 cells is shown together with immunofluorescence staining of SRSF2 (red) and SRRM2 (blue). Scale bar: 10 µm. (E) The size distributions of HiNoCo-body in siControl (n=315), siHSF1#1 (n=320), or siHSF1#2 (n=262) transfected cells were analyzed. The box represents the 25–75th percentiles, and the median is indicated. The whiskers show the values within 1.5× of the interquartile range. *P*-values were obtained by Wilcoxon rank sum test.

inhibitor of phase-separated structures but not solid protein assemblies (Kroschwald et al., 2017). HiNoCo body formation was observed in more than 80% of nuclei and 1,6-hexanediol treatment disrupted HiNoCo body formation in 80% of nuclei (Fig. 5B). However, this treatment did not affect *MALAT1* localization in nuclear speckles in non-heat-treated cells nor the formation of nuclear speckles themselves in both non-treated and heat-treated cells (Fig. 5A; Fig. S5). In contrast, 2,5-hexanediol, which does not disrupt phase-separated structures (Lin et al., 2016), did not affect the localization of *MALAT1* in both non-treated and heat-treated cells (Fig. 5A; Fig. S5). Finally, the expression level of *MALAT1* was not altered by 1,6-hexanediol and 2,5-hexanediol (Fig. 5C). These results suggest that HiNoCo body is a phase-separated structure.

DISCUSSION

In this study, we showed that *MALAT1* translocates thermo-responsively and reversibly to a distinct nuclear granular structure in an HSF1-independent manner in response to heat shock. We named this distinct nuclear granular structure the HiNoCo body. The HiNoCo body is a novel nuclear body that is evolutionarily conserved in human and mouse cells, and is distinct from nuclear stress body, which is formed only in primate cells upon heat shock at the primate-specific pericentromeric satellite III arrays near their own loci in HSF1-dependent manner (Jolly et al., 2004; Rizzi et al., 2004). Of note, we found that *MALAT1* knockout reduced cell proliferation after heat-shock treatment, suggesting that HiNoCo body is important for the HSR.

Journal of Cell Science (2021) 134, jcs253559. doi:10.1242/jcs.253559

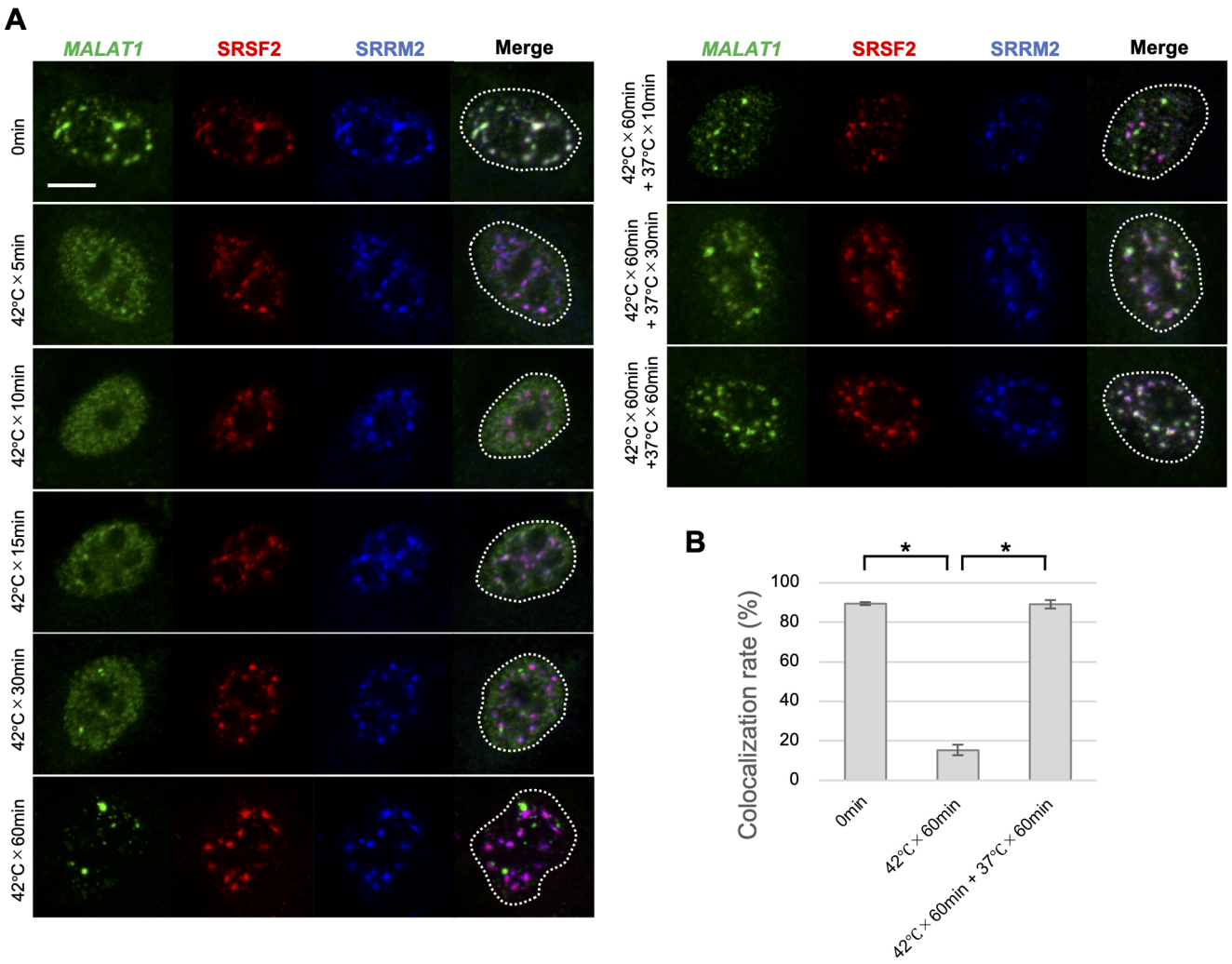

Fig. 4. Time course of HiNoCo body formation after heat shock. (A) Representative images of nuclear speckle proteins and *MALAT1* in A549 cells. A549 cells were incubated at 42°C for 0, 5, 10, 15, 30 or 60 min, or at 42°C for 60 min, followed by 37°C for 10, 30 or 60 min. A549 cells were subjected to RNA-FISH for *MALAT1* (green), and to immunofluorescence staining for SRSF2 (red) and SRRM2 (blue). Dotted lines outline the nucleus. Scale bar: 10 µm. (B) The colocalization rate of *MALAT1* and SRSF2 in heat-treated A549 cells shown in FA was determined using LAS-AF software (Leica microsystems). Values represent the mean±s.d. of four images (20–30 cells per image). **P*<0.01 (Welch's *t*-test).

The number of granules containing either *Malat1* or Srrm2 in MEFs (Fig. 1B) and in C17.2 cells (Fig. S1C) tended to be more numerous under heat shock, and their size was smaller than nuclear speckles in non-treated cells. These differences may be due to the difference in the HSR system between humans and mice, such as the presence or absence of nuclear stress bodies. Upon heat shock stress, the number of HiNoCo bodies was reduced compared with nuclear speckles (Fig. S2B). This may reflect the difference in components present in nuclear speckles and HiNoCo bodies.

Our time course analysis of HiNoCo body formation revealed that *MALAT1* diffused from nuclear speckles to the nucleoplasm and formed small granules that increased in size (Fig. 4). PCBP1 depletion prevented *MALAT1* disassociation with nuclear speckles during heat shock (Fig. S3), suggesting that PCBP1 is required for the release of *MALAT1* from nuclear speckles (Fig. 5D). Moreover, we found that *MALAT1* could not form HiNoCo bodies in the presence of a transcriptional inhibitor (Fig. S1G), suggesting that active transcription is important for the formation of HiNoCo body. Based on these results, we propose a model in which *MALAT1* is released from nuclear speckles by a PCBP-mediated pathway soon after heat shock, and *MALAT1* localizes into the HiNoCo body, in a manner that is dependent on active transcription (Fig. 5D). Of note, there is a possibility that the diffusion of *MALAT1* into the nucleoplasm reflects transcriptional inhibition by heat shock stress for the following reasons: (1) heat shock causes global transcriptional repression and certain genes are downregulated rapidly after heat shock treatment (Mahat et al., 2016); and (2) transcriptional inhibition prevents the nuclear speckle localization of *MALAT1* (Bernard et al., 2010; Tani et al., 2012b).

Heat shock also enhances the formation of stress granules, which are phase-separated membraneless compartments in the cytoplasm (Protter and Parker, 2016). Stress granules in the cytoplasm serve as a sensing system for heat shock or pH stress using the physicochemical properties of liquid–liquid phase separation in yeast (Franzmann et al., 2018; Kroschwald et al., 2018; Riback et al., 2017). The sensitivity of HiNoCo body to 1,6-hexanediol supports the idea that HiNoCo body is a phase-separated membraneless granule, like stress granules in cytoplasm (Fig. 5A), although 1,6-hexanediol is widely used but not necessarily definitive for liquid-liquid phase separation (Alberti et al., 2019). In addition, we speculate that HiNoCo body

Journal of Cell Science (2021) 134, jcs253559. doi:10.1242/jcs.253559

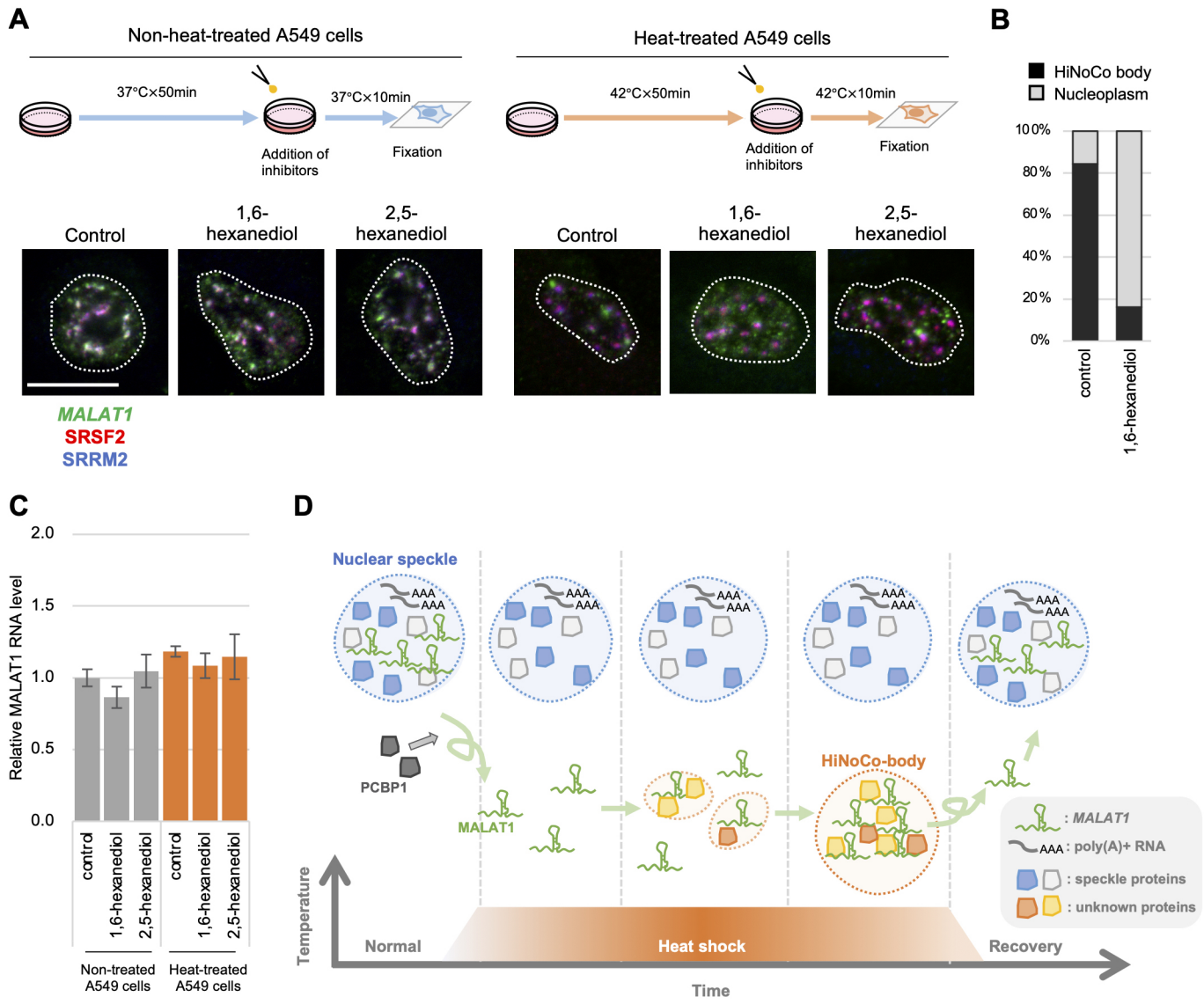

Fig. 5. Inhibitors of liquid-liquid phase separation disrupted HiNoCo body formation. (A) Representative images of *MALAT1* and nuclear speckle proteins in non-heat-treated and heat-treated A549 cells treated with 1,6-hexianediole or 2,5-hexianediole. 1,6- or 2,5-hexianediole (final concentration 50 mM) was added to non-heat-treated (incubated at 37°C) and heat-treated (incubated at 42°C for 50 min) A549 cells, and incubated for another 10 min. Fixed cells were subjected to RNA-FISH and immunostaining analysis. RNA-FISH of *MALAT1* (green) in A549 cells is shown together with immunofluorescence staining of SRSF2 (red) and SRRM2 (blue). Dotted lines outline the nucleus. Scale bar: 10 µm. (B) The percentage of nuclei with HiNoCo bodies in non-treated (*n*=102) and 1,6-hexanediol-treated (*n*=98) A549 cells. (C) qRT-PCR was used to determine the relative *MALAT1* expression level in A549 cells treated with 1,6- or 2,5-hexianediole. *MALAT1* level was normalized to *GAPDH* mRNA. Mean±s.d. was determined for biological triplicates. (D) A model of the HiNoCo body formation in response to heat shock. In normal conditions, *MALAT1* localizes in nuclear speckles like poly(A)+ RNA. Heat shock initially induces diffusion of *MALAT1* from the nuclear speckles to the nucleoplasm, and then it starts forming a small granule-like structure (HiNoCo body). The size of the HiNoCo body increases over time under heat shock. *MALAT1* returns to nuclear speckles after the temperature is shifted from heat shock to normal.

formation may act as a biosensor in the nucleus to monitor temperature changes through the phase separation phenomenon. Further analysis of HiNoCo body formation may contribute to elucidating the cellular stress response system.

MATERIALS AND METHODS

Cell cultures

MEFs (kindly supplied by Dr Yumiko Kawamura, University of Tokyo, Japan), A549 cells, A549 *MALAT1* knockout cells (Gutschner et al., 2013) and C17.2 cells (kindly provided by Dr Yasunobu Uchijima, University of Tokyo, Japan) were cultured in Dulbecco's modified Eagle's medium (DMEM) supplemented with 10% heat-inactivated fetal bovine serum and antibiotics at 37°C in a humidified incubator with 5% CO_2. To induce heat shock stress, MEFs, A549 and C17.2 cells were placed in a humidified incubator at 42°C with 5% CO_2 for the indicated periods. For sodium arsenate treatment, 0.5 mM of sodium arsenate (Sigma-Aldrich, St Louis, MO, USA, #S7400) was added to A549 cells and incubated in a humidified incubator with 5% CO_2 at 37°C for 1 h. To induce ultraviolet (UV) stress, A549 cells were irradiated by 10 J/m^2 UV light and placed in a humidified incubator with 5% CO_2 at 37°C for 8 h. For X-ray irradiation, A549 cells were exposed to 5 Gy of X-rays and incubated in a humidified incubator with 5% CO_2 at 37°C for 2 h after irradiation. To inhibit transcription, 2 µg/ml of actinomycin D (Sigma-Aldrich, #A9415) was added to A549 cells that were incubated in a humidified incubator with 5% CO_2 at 37°C for 27 h. For inhibition of liquid–liquid phase separation, 1,6-hexanediol

(Wako, Osaka, Japan, #087-00432) or 2,5-hexanediol (Sigma-Aldrich, #11904-10G) (final concentration 50 mM) was added to non-treated (incubated at 37°C) and heat-treated (incubated at 42°C for 50 min) A549 cells for 10 min.

Reverse transcription quantitative real-time PCR

Total RNA was extracted from cells with RNAiso Plus (#9109, TaKaRa Bio Inc., Shiga, Japan) according to the manufacturer's instructions. Isolated RNA was reverse transcribed into cDNA using PrimeScript RT Master Mix (Perfect Real Time; #RR036B, TaKaRa Bio Inc.). The cDNA was amplified using the primer set listed in Table S1. SYBR Premix Ex Taq2 (Perfect Real Time; #RR820W, TaKaRa Bio Inc.) was used according to the manufacturer's instructions. qRT-PCR analysis was performed using a Thermal Cycler Dice Real Time system (TaKaRa Bio Inc.), according to the manufacturer's instructions.

Northern blot analysis

Total RNA was extracted from non-treated or heat-treated (42°C for 1 h) cells with RNAiso Plus according to the manufacturer's instructions. Total RNA (10 µg) was separated on a 1.1% (w/v) agarose gel containing 0.08% formaldehyde and transferred to a positively charged nylon membrane (Millipore, Bedford, MA, USA). After UV cross-linking, blots were hybridized to previously described ^{32}P-labeled riboprobes (Tano et al., 2010) at 52°C overnight in Ultrasensitive Hybridization Buffer (Applied Biosystems, Foster City, CA, USA). An autoradiograph was captured and quantified using an FLA9000 biomolecular imager (FUJIFILM, Tokyo, Japan).

BrU pulse-chase analysis

BrU pulse-chase analysis (BRIC-qPCR analysis) was performed as described previously (Tani et al., 2012a). Briefly, A549 cells were incubated at 37°C in the presence of 150 µM BrU (Wako, Osaka, Japan) for 24 h in a humidified incubator with 5% CO_2. After replacing the BrU-containing medium with BrU-free medium, cells were incubated at 37°C or 42°C for 1 h. Cells were harvested and total RNA was isolated using RNAiso Plus (TaKaRa), followed by isolation of BrU-labeled RNA by anti-BrdU mouse antibody (clone 2B1, MBL, Nagoya, Japan). The isolated RNA was quantified by qRT-PCR.

Cell viability assay

Cell viability was assessed using a Cell Counting Kit-8 (Dojindo, Kumamoto, Japan) at 0, 24, 48, and 72 h after heat shock treatment (42°C, 1 h). The procedures were performed according to the manufacturer's instructions.

RNA-FISH

Cells cultured on cover glasses in 12-well plates were washed with PBS(-) (PBS without Ca^{2+} and Mg^{2+}) and fixed with 4% PFA in PBS(-) for 20 min at room temperature. Then, the cover glasses were washed twice with PBS(-) and permeabilized with 0.5% Triton X-100 in PBS(-) for 5 min at 4°C. The cover glasses were washed twice with PBS(-) and incubated in hybridization buffer [50% formamide, 1× Denhardt's solution, 1× SSC, 10 mM EDTA, 0.01% Tween 20, 0.1 mg/ml yeast tRNA (Sigma-Aldrich, #R8508)] for 2 h at 55°C. Digoxigenin (DIG)-labeled antisense RNA probe mixed in hybridization buffer was added to the cover glasses, and incubated for 16 h at 55°C. The cover glasses were washed twice with wash buffer (50% formamide, 2× SSC and 0.01% Tween 20) for 15 min at 55°C, and then incubated in 5 µg/ml RNaseA (Sigma-Aldrich, #R4642) in TNET (50 mM Tris-HCl, pH 7.4, 140 mM NaCl, 5 mM EDTA, 0.01% Triton X-100) for 30 min at 37°C. Subsequently, the cover glasses were incubated in 2× SSC plus 0.01% Tween 20 for 15 min at 55°C and washed twice with 0.1× SSC plus 0.01% Tween 20 for 15 min at 55°C. After blocking with 1% BSA in PBS(-) with 0.01% Tween 20 for 1 h at room temperature, the cover glasses were incubated in 1% BSA in PBS(-) with 0.01% Tween 20 containing anti-DIG sheep antibody (Roche, Mannheim, Germany) and antibodies against the proteins of interest (Table S2). After washing with PBS(-) plus 0.2% Tween 20, a solution of 1% BSA in PBS(-) with 0.01% Tween 20 with Alexa Fluor 488-, Alexa Fluor 555-, or Alexa Fluor 647-conjugated secondary antibodies was added to the cover glasses for 1 h at room temperature. After washing with PBS(-) plus 0.2% Tween 20, the cover glasses were incubated in DAPI in PBS(-) for 10 min at room temperature. The cover glasses were mounted with Prolong Gold (#P36934, Invitrogen, Carlsbad, CA, USA).

To prepare the template cDNA for the synthesis of the RNA probe, the *MALAT1* fragment (1930–5644 nt in NR_002819.4) was subcloned into pSC-B vector (Stratagene, La Jolla, CA, USA). A DIG-labeled *MALAT1* RNA probe was synthesized using DIG RNA-labeling mix (#11277073910, Roche) and T3 RNA polymerase (#11031163001, Roche) according to the manufacturer's instructions. For *in situ* hybridization of nuclear poly(A)+ RNA, an Alexa Fluor 594-conjugated oligonucleotide dT34 probe (previously described in Miyagawa et al., 2012)] was used. The antibodies used are listed in Table S2.

The images were acquired with a Leica TCS SP5 confocal microscope (Leica microsystems, Wetzlar, Germany). More than 100 cells were observed in each experiment. To examine the colocalization of *MALAT1* and *SRSF2*, the colocalization rate was determined using the colocalization tool in the LAS-AF software (Leica microsystems) under the following conditions and calculations: threshold 30%, background 35%; colocalization rate (%)=area colocalization/area foreground, and area foreground=area image – area background. To analyze the number or size of HiNoCo bodies, images were taken as *Z*-stacks and projected in one plane with maximum intensity using Fiji/ImageJ (Image/Stack/Z Project). *Z*-projected images were binarized using Fiji/ImageJ (Image/Adjust/threshold, threshold 30) and the size of HiNoCo bodies were measured by the Analyze particle tool in Fiji/ImageJ.

High-resolution images were acquired with a Leica STELLARIS5 confocal microscope (Leica Microsystems, Wetzlar, Germany) with the following conditions: objective lens 63×oil lens, pinhole 0.5 AU; and pixel size 29 nm×29 nm. The images were submitted to automated internal Leica Lightning deconvolution software with the default setting.

siRNA

The siRNA sequences are listed in Table S3. To improve knockdown efficiency, siRNAs were transfected into cells sequentially using Lipofectamine RNAi MAX (Invitrogen), according to the manufacturer's instructions. Briefly, siRNA duplexes (final concentration 10 nM) were transfected into 4×10^4 cells (first transfection), followed by incubation for 6 h at 37°C and 5% CO_2. After changing the medium, the cells were incubated overnight at 37°C and 5% CO_2. The following day, siRNA duplexes (final concentration 10 nM) were transfected into the cells again (second transfection), followed by incubation for 6 h at 37°C and 5% CO_2. After changing the medium, the cells were incubated for 24 h at 37°C and 5% CO_2.

Western blot analysis

Total protein extracts were prepared in RIPA buffer [50 mM Tris-HCl pH 8, 150 mM NaCl, 1 mM EDTA, 0.1% SDS, 1% Triton X-100, 0.1% DOC, and protease inhibitor cocktail (#P8340, Sigma-Aldrich)] and separated on 10% SDS-PAGE gels. The proteins were transferred onto a PVDF membrane (Millipore). The membrane was blocked with 3% BSA in Tris-buffered saline containing 0.1% Triton X-100 (TBST) and incubated with anti-HSF1 or anti-GAPDH antibody (Table S2) for 1 h at room temperature. After washing the membrane with TBST, the membrane was incubated with horseradish peroxidase (HRP)-linked secondary antibodies for 1 h at room temperature. The proteins were visualized using Immobilon western chemiluminescent HRP substrate (#WBLUF0500, Millipore) and LAS-4000UVmini Luminescent Image Analyzer (FUJIFILM), according to the manufacturer's instructions.

Statistical analysis

The qRT-PCR analysis was performed on biological triplicates. The statistical significance was assessed by Welch's *t*-test with Bonferroni correction.

Acknowledgements

We thank Dr Yoshihiro Urade and Dr Kenzui Taniue for fruitful suggestions. MEFs were kindly supplied by Dr Yumiko Kawamura (University of Tokyo, Japan). C17.2 cells were kindly provided by Dr Yasunobu Uchijima (University of Tokyo, Japan).

We thank Michal Bell, PhD, and J. Ludovic Croxford, PhD, from Edanz Group (https://en-author-services.edanz.com/ac) for editing a draft of the manuscript.

Competing interests
The authors declare no competing or financial interests.

Author contributions
Conceptualization: R.O.-M., N.A.; Investigation: R.O.-M., Y.K., Y.O., T.G., S.D.; Writing - original draft: R.O.-M.; Writing - review & editing: N.A.; Supervision: N.A.; Project administration: N.A.; Funding acquisition: R.O.-M., N.A.

Funding
This work was supported by grants from The Ministry of Education, Culture, Sports, Science and Technology (MEXT) KAKENHI (16H06743, 18H02570, 18KT0016, 20H04838), Takeda Science Foundation, Uehara Memorial Foundation, and Princess Takamatsu Cancer Research Fund.

Peer review history
The peer review history is available online at
https://journals.biologists.com/jcs/article-lookup/doi/10.1242/jcs.253559

References
Alberti, S., Gladfelter, A. and Mittag, T. (2019). Considerations and challenges in studying liquid-liquid phase separation and biomolecular condensates. *Cell* **176**, 419-434. doi:10.1016/j.cell.2018.12.035

Arun, G., Aggarwal, D. and Spector, D. L. (2020). MALAT1 long non-coding RNA: functional implications. *Noncoding RNA* **6**, 22. doi:10.3390/ncrna6020022

Banani, S. F., Lee, H. O., Hyman, A. A. and Rosen, M. K. (2017). Biomolecular condensates: organizers of cellular biochemistry. *Nat. Rev. Mol. Cell Biol.* **18**, 285-298. doi:10.1038/nrm.2017.7

Bernard, D., Prasanth, K. V., Tripathi, V., Colasse, S., Nakamura, T., Xuan, Z., Zhang, M. Q., Sedel, F., Jourdren, L., Coulpier, F. et al. (2010). A long nuclear-retained non-coding RNA regulates synaptogenesis by modulating gene expression. *EMBO J.* **29**, 3082-3093. doi:10.1038/emboj.2010.199

Clemson, C. M., Hutchinson, J. N., Sara, S. A., Ensminger, A. W., Fox, A. H., Chess, A. and Lawrence, J. B. (2009). An architectural role for a nuclear noncoding RNA: NEAT1 RNA is essential for the structure of paraspeckles. *Mol. Cell* **33**, 717-726. doi:10.1016/j.molcel.2009.01.026

Cotto, J. J., Fox, S. G. and Morimoto, R. I. (1997). HSF1 granules: a novel stress-induced nuclear compartment of human cells. *J. Cell Sci.* **110**, 2925-2934. doi:10.1242/jcs.110.23.2925

Eißmann, M., Gutschner, T., Hämmerle, M., Günther, S., Caudron-Herger, M., Groß, M., Schirmacher, P., Rippe, K., Braun, T., Zörnig, M. et al. (2012). Loss of the abundant nuclear non-coding RNA MALAT1 is compatible with life and development. *RNA Biol.* **9**, 1076-1087. doi:10.4161/rna.21089

Engreitz, J. M., Ollikainen, N. and Guttman, M. (2016). Long non-coding RNAs: Spatial amplifiers that control nuclear structure and gene expression. *Nat. Rev. Mol. Cell Biol.* **17**, 756-770. doi:10.1038/nrm.2016.126

Fei, J., Jadaliha, M., Harmon, T. S., Li, I. T. S., Hua, B., Hao, Q., Holehouse, A. S., Reyer, M., Sun, Q., Freier, S. M. et al. (2017). Quantitative analysis of multilayer organization of proteins and RNA in nuclear speckles at super resolution. *J. Cell Sci.* **130**, 4180-4192. doi:10.1242/jcs.206854

Franzmann, T. M., Jahnel, M., Pozniakovsky, A., Mahamid, J., Holehouse, A. S., Nüske, E., Richter, D., Baumeister, W., Grill, S. W., Pappu, R. V. et al. (2018). Phase separation of a yeast prion protein promotes cellular fitness. *Science (80-.)* **359**, eaao5654. doi:10.1126/science.aao5654

Gutschner, T., Hämmerle, M., Eißmann, M., Hsu, J., Kim, Y., Hung, G., Revenko, A., Arun, G., Stentrup, M., Groß, M. et al. (2013). The noncoding RNA MALAT1 is a critical regulator of the metastasis phenotype of lung cancer cells. *Cancer Res.* **73**, 1180-1189. doi:10.1158/0008-5472.CAN-12-2850

Hirose, T., Yamazaki, T. and Nakagawa, S. (2019). Molecular anatomy of the architectural NEAT1 noncoding RNA: the domains, interactors, and biogenesis pathway required to build phase-separated nuclear paraspeckles. *Wiley Interdiscip. Rev. RNA* **10**, 1-13. doi:10.1002/wrna.1545

Hutchinson, J. N., Ensminger, A. W., Clemson, C. M., Lynch, C. R., Lawrence, J. B. and Chess, A. (2007). A screen for nuclear transcripts identifies two linked noncoding RNAs associated with SC35 splicing domains. *BMC Genomics* **8**, 1-16. doi:10.1186/1471-2164-8-1

Hyman, A. A., Weber, C. A. and Jülicher, F. (2014). Liquid-liquid phase separation in biology. *Annu. Rev. Cell Dev. Biol.* **30**, 39-58. doi:10.1146/annurev-cellbio-100913-013325

Imamura, K., Imamachi, N., Akizuki, G., Kumakura, M., Kawaguchi, A., Nagata, K., Kato, A., Kawaguchi, Y., Sato, H., Yoneda, M. et al. (2014). Long noncoding RNA NEAT1-dependent SFPQ relocation from promoter region to paraspeckle mediates IL8 expression upon immune stimuli. *Mol. Cell* **53**, 393-406. doi:10.1016/j.molcel.2014.01.009

Imamura, K., Takaya, A., Ishida, Y., Fukuoka, Y., Taya, T., Nakaki, R., Kakeda, M., Imamachi, N., Sato, A., Yamada, T. et al. (2018). Diminished nuclear RNA decay upon Salmonella infection upregulates antibacterial noncoding RNA s. *EMBO J.* **37**, 1-15. doi:10.15252/embj.201797723

Ji, P., Diederichs, S., Wang, W., Böing, S., Metzger, R., Schneider, P. M., Tidow, N., Brandt, B., Buerger, H., Bulk, E. et al. (2003). MALAT-1, a novel noncoding RNA, and thymosin β4 predict metastasis and survival in early-stage non-small cell lung cancer. *Oncogene* **22**, 8031-8041. doi:10.1038/sj.onc.1206928

Jolly, C., Usson, Y. and Morimoto, R. I. (1999). Rapid and reversible relocalization of heat shock factor 1 within seconds to nuclear stress granules. *Proc. Natl. Acad. Sci. USA* **96**, 6769-6774. doi:10.1073/pnas.96.12.6769

Jolly, C., Metz, A., Govin, J., Vigneron, M., Turner, B. M., Khochbin, S. and Vourc'h, C. (2004). Stress-induced transcription of satellite III repeats. *J. Cell Biol.* **164**, 25-33. doi:10.1083/jcb.200306104

Kroschwald, S., Maharana, S. and Simon, A. (2017). Hexanediol: a chemical probe to investigate the material properties of membrane-less compartments. *Matters* doi:10.19185/matters.201702000010

Kroschwald, S., Munder, M. C., Maharana, S., Franzmann, T. M., Richter, D., Ruer, M., Hyman, A. A. and Alberti, S. (2018). Different material states of Pub1 condensates define distinct modes of stress adaptation and recovery. *Cell Rep.* **23**, 3327-3339. doi:10.1016/j.celrep.2018.05.041

Li, J., Labbadia, J. and Morimoto, R. I. (2017). Rethinking HSF1 in stress, development, and organismal health. *Trends Cell Biol.* **27**, 895-905. doi:10.1016/j.tcb.2017.08.002

Lin, Y., Mori, E., Kato, M., Xiang, S., Wu, L., Kwon, I. and McKnight, S. L. (2016). Toxic PR poly-dipeptides encoded by the C9orf72 repeat expansion target LC domain polymers. *Cell* **167**, 789-802.e12. doi:10.1016/j.cell.2016.10.003

Mahat, D. B., Salamanca, H. H., Duarte, F. M., Danko, C. G. and Lis, J. T. (2016). Mammalian heat shock response and mechanisms underlying its genome-wide transcriptional regulation. *Mol. Cell* **62**, 63-78. doi:10.1016/j.molcel.2016.02.025

Miyagawa, R., Tano, K., Mizuno, R., Nakamura, Y., Ijiri, K., Rakwal, R., Shibato, J., Masuo, Y., Mayeda, A., Hirose, T., Akimitsu, N. et al. (2012). Identification of cis- and trans-acting factors involved in the localization of MALAT-1 noncoding RNA to nuclear speckles. *RNA* **18**, 738-751. doi:10.1261/rna.028639.111

Nakagawa, S., Ip, J. Y., Shioi, G., Tripathi, V., Zong, X., Hirose, T. and Prasanth, K. V. (2012). Malat1 is not an essential component of nuclear speckles in mice. *RNA* **18**, 1487-1499. doi:10.1261/rna.033217.112

Ninomiya, K., Adachi, S., Natsume, T., Iwakiri, J., Terai, G., Asai, K. and Hirose, T. (2020). Lnc RNA –dependent nuclear stress bodies promote intron retention through SR protein phosphorylation. *EMBO J.* **39**, 1-20. doi:10.15252/embj.2019102729

Protter, D. S. W. and Parker, R. (2016). Principles and properties of stress granules. *Trends Cell Biol.* **26**, 668-679. doi:10.1016/j.tcb.2016.05.004

Riback, J. A., Katanski, C. D., Kear-Scott, J. L., Pilipenko, E. V., Rojek, A. E., Sosnick, T. R. and Drummond, D. A. (2017). Stress-triggered phase separation is an adaptive, evolutionarily tuned response. *Cell* **168**, 1028-1040.e19. doi:10.1016/j.cell.2017.02.027

Richter, K., Haslbeck, M. and Buchner, J. (2010). The heat shock response: life on the verge of death. *Mol. Cell* **40**, 253-266. doi:10.1016/j.molcel.2010.10.006

Rizzi, N., Denegri, M., Chiodi, I., Corioni, M., Valgardsdottir, R., Cobianchi, F., Riva, S. and Biamonti, G. (2004). Transcriptional activation of a constitutive heterochromatic domain of the human genome in response to heat shock. *Mol. Biol. Cell* **15**, 543-551. doi:10.1091/mbc.e03-07-0487

Sharma, A., Takata, H., Shibahara, K., Bubulya, A. and Bubulya, P. A. (2010). Son is essential for nuclear speckle organization and cell cycle progression. *Mol. Biol. Cell* **21**, 650-663. doi:10.1091/mbc.e09-02-0126

Shirahama, S., Miki, A., Kaburaki, T. and Akimitsu, N. (2020). Long non-coding RNAs involved in pathogenic infection. *Front. Genet.* **11**, 454. doi:10.3389/fgene.2020.00454

Tani, H., Mizutani, R., Salam, K. A., Tano, K., Ijiri, K., Wakamatsu, A., Isogai, T., Suzuki, Y. and Akimitsu, N. (2012a). Genome-wide determination of RNA stability reveals hundreds of short-lived noncoding transcripts in mammals (Genome Research (2012) 22, (947-956)). *Genome Res.* **22**, 1382. doi:10.1101/gr.130559.111

Tani, H., Imamachi, N., Salam, K. A., Mizutani, R., Ijiri, K., Irie, T., Yada, T., Suzuki, Y. and Akimitsu, N. (2012b). Identification of hundreds of novel UPF1 target transcripts by direct determination of whole transcriptome stability. *RNA Biol.* **9**, 1370-1379. doi:10.4161/rna.22360

Tano, K., Mizuno, R., Okada, T., Rakwal, R., Shibato, J., Masuo, Y., Ijiri, K. and Akimitsu, N. (2010). MALAT-1 enhances cell motility of lung adenocarcinoma cells by influencing the expression of motility-related genes. *FEBS Lett.* **584**, 4575-4580. doi:10.1016/j.febslet.2010.10.008

Tano, K., Onoguchi-Mizutani, R., Yeasmin, F., Uchiumi, F., Suzuki, Y., Yada, T. and Akimitsu, N. (2018). Identification of minimal p53 promoter region regulated by MALAT1 in human lung adenocarcinoma cells. *Front. Genet.* **8**, 208. doi:10.3389/fgene.2017.00208

Trinklein, N. D., Chen, W. C., Kingston, R. E. and Myers, R. M. (2004). Transcriptional regulation and binding of heat shock factor 1 and heat shock factor 2 to 32 human heat shock genes during thermal stress and differentiation. *Cell Stress Chaperones* **9**, 21-28. doi:10.1379/1466-1268(2004)009<0021:TRABOH>2.0.CO;2

Tripathi, V., Ellis, J. D., Shen, Z., Song, D. Y., Pan, Q., Watt, A. T., Freier, S. M., Bennett, C. F., Sharma, A., Bubulya, P. A. et al. (2010). The nuclear-retained

noncoding RNA MALAT1 regulates alternative splicing by modulating SR splicing factor phosphorylation. *Mol. Cell* **39**, 925-938. doi:10.1016/j.molcel.2010.08.011

Tripathi, V., Song, D. Y., Zong, X., Shevtsov, S. P., Hearn, S., Fu, X. D., Dundr, M. and Prasanth, K. V. (2012). SRSF1 regulates the assembly of pre-mRNA processing factors in nuclear speckles. *Mol. Biol. Cell* **23**, 3694-3706. doi:10.1091/mbc.e12-03-0206

Wang, C., Lu, T., Emanuel, G., Babcock, H. P. and Zhuang, X. (2019). Imaging-based pooled CRISPR screening reveals regulators of lncRNA localization. *Proc. Natl. Acad. Sci. USA* **166**, 10842-10851. doi:10.1073/pnas.1903808116

Wheeler, J. R., Matheny, T., Jain, S., Abrisch, R. and Parker, R. (2016). Distinct stages in stress granule assembly and disassembly. *Elife* **5**, e18413. doi:10.7554/eLife.18413

Wilusz, J. E., Freier, S. M. and Spector, D. L. (2008). 3′ End processing of a long nuclear-retained noncoding RNA yields a tRNA-like cytoplasmic RNA. *Cell* **135**, 919-932. doi:10.1016/j.cell.2008.10.012

Zhang, B., Arun, G., Mao, Y. S., Lazar, Z., Hung, G., Bhattacharjee, G., Xiao, X., Booth, C. J., Wu, J., Zhang, C. et al. (2012). The lncRNA malat1 is dispensable for mouse development but its transcription plays a cis-regulatory role in the adult. *Cell Rep.* **2**, 111-123. doi:10.1016/j.celrep.2012.06.003